Journal of Electrical Engineering & Technology Vol. 7, No. 4, pp. 589~595, 2012 **589**
http://dx.doi.org/10.5370/JEET.2012.7.4.589

Frequency-dependent grounding impedance of the counterpoise based on the dispersed currents

Jong-Hyuk Choi†, Bok-Hee Lee* and Seung-Kwon Paek**

Abstract – When surges and electromagnetic pulses from lightning or power conversion devices are considered, it is desirable to evaluate grounding system performance as grounding impedance. In the case of large-sized grounding electrodes or long counterpoises, the grounding impedance is increased with increasing the frequency of injected current. The grounding impedance is increased by the inductance of grounding electrodes. This paper presents the measured results of frequency-dependent grounding impedance and impedance phase as a function of the length of counterpoises. In order to analyze the frequency-dependent grounding impedance of the counterpoises, the frequency-dependent current dissipation rates were measured and simulated by the distributed parameter circuit model reflecting the frequency-dependent relative resistivity and permittivity of soil. As a result, the ground current dissipation rate is proportional to the soil resistivity near the counterpoises in a low frequency. On the other hand, the ground current dissipation near the injection point is increased as the frequency of injected current increases. Since the high frequency ground current cannot reach the far end of long counterpoise, the grounding impedance of long counterpoise approaches that of the short one in the high frequency. The results obtained from this work could be applied in design of grounding systems.

Keywords: Grounding impedance, Ground current dissipation, Distributed parameter circuit model, Counterpoise, Soil resistivity

1. Introduction

Grounding systems of electric power and industrial systems play an important role during perturbation where the behavior of the electrical systems and safety of technicians and general public are concerned [1]. It is also one of the most important parts of lightning protection systems for complex information technology equipment [2]. According to the electrotechnical regulations of Korea and other countries, the grounding system performance is evaluated by means of the ground resistance measured at the low frequency [3,4]. To satisfy the designated value of the ground resistance, a grounding system is extremely over-extended. However, high frequency characteristics of grounding systems are quite different from those at a low frequency [5-7]. Because the impedance of grounding systems includes resistive, inductive and capacitive components at a high frequency, the grounding impedance rather than the ground resistance should be defined and evaluated. A lot of literature present the effective length of grounding electrodes and it means the expanded length and area of grounding electrode systems have a little effect to reduce the grounding impedance at a high frequency [2], [8,9]. Grounding impedance consists of resistive, capacitive and inductive components and the ground resistance is the real part of the grounding impedance measured at a low frequency [9]. This paper describes the experimental and simulated results of the frequency-dependent grounding impedance as functions of the length of counterpoise and the current dissipation rates of dispersing into the soil near the grounding electrode. The relation between the grounding impedance and ground current dissipation rates were analyzed. Also the results of the grounding impedance and ground current dissipation rates simulated by using the distributed parameter circuit model were presented, and the comparison between the theoretical calculated and measured results was discussed.

† Corresponding Author: Korea Electrotechnology Research Institute(KERI), Korea. (choijh@keri.re.kr)
* School of Electrical Engineering, Inha University, Korea. (bhlee@inha.ac.kr)
** Department of electronics and intelligent robotics Engineering, Inje University, Kimhae, Korea. (elecpsk@inje.ac.kr).
Received: January 10, 2011; Accepted: March 5, 2012

2. Methodology

2.1 Experimental method

The ground current is classified into two components: the leakage transversal current spread into the soil and the longitudinal current transferred to the remaining electrode length [9]. In this paper, the counterpoise with the radius of 2.82 mm was installed in depth of 0.5 m, and the length of the counterpoise is adjusted to investigate the frequency-dependent grounding impedance and the ground current dissipation rate. The current dispersed into the soil at every

10 m section of the grounding electrode was measured for the counterpoise of 50 m. The grounding impedance is also measured as functions of the frequency of test current and the length of counterpoise. Before installing the counterpoise, the soil structure of the test site is surveyed by the dipole-dipole method with the earth resistivity analyzer (Syscal-pro). Fig. 1 shows the profile of the soil structure of the test site where the counterpoise was installed. The ground resistance is significantly affected the soil resistivity near the grounding electrodes [10]. The localized soil resistivity is different depending on the site where the counterpoise is buried, as shown in Fig. 1. In the case of the soil structures nearby the counterpoise, the localized soil resistivity of the 10 m sections of 0-20 m, 20-30 m, 40-50 m is lower than that of other parts of the counterpoise. The ground resistance of the counterpoise of 50 m long is 8.55 Ω and the apparent soil resistivity reversely calculated from Eq. (1) is 205.34 Ω·m [11].

$$\rho = \frac{R \cdot \pi l}{\ln \frac{2l}{\sqrt{2rt}} - 1} \tag{1}$$

where,

R is the ground resistance of the counterpoise.

l , r are the length and radius of the counterpoise, respectively.

t is the buried depth of the counterpoise.

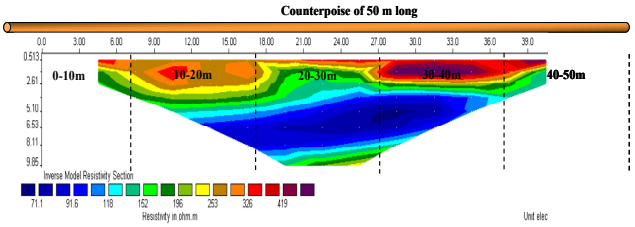

Fig. 1. Two-dimensional map of the soil structure of the test site where the counterpoise of 50 m long is buried

Fig. 2 illustrates the configuration of the experimental setup to measure the ground current dissipation rates and the grounding impedance. The current dispersed into the earth in every 10 m sections of the counterpoise are evaluated from the detected current waveforms at every 10 m point and the current injection point of the counterpoise. The teat current is supplied by the function generator with a frequency bandwidth of 80 MHz and power amplifier with a frequency bandwidth of 250 MHz. Current transformers (Pearson 3525) are installed at every 10 m point of the counterpoise to observe the ground current dissipated into the earth each section of the counterpoise. The detected signal is transmitted to a digital storage oscilloscope with a 2.5 Giga sampling rate and the frequency bandwidth of 1 GHz.

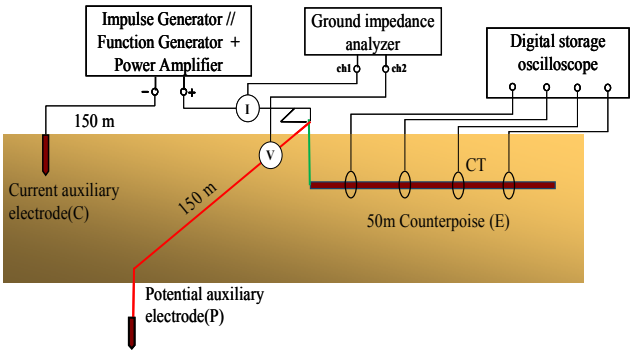

Fig. 2. Arrangement of the experimental setup

The frequency-dependent grounding impedance and impedance phase are measured as a function of the every 10 m length of the counterpoise. The revised fall-of-potential method arraying the current and potential auxiliary electrodes at an angle of 90° recommended by IEEE Standard 81.2 is adapted to measure the grounding impedance [12]. The current and potential auxiliary electrodes are installed at the location of 150 m far away the counterpoise to be measured. For a ground electrode installed in homogeneous earth, when P_1 and C_1 are greater than the length of the measured grounding electrode and the angle between the current and potential probes is 90° , the measurement error, Z_e , due to earth mutual impedance is given by

$$Z_e = \frac{\rho}{2\pi}\left[\frac{1}{\sqrt{P_1^2 + C_1^2}} - \frac{1}{C_1} - \frac{1}{P_1}\right] \tag{2}$$

where,

C_1 is the spacing between the measured ground electrode and current probe.

P_1 is the spacing between the measured ground electrode and potential probe.

when $P_1 = C_1 = 150$ m, the measurement earth mutual error due to impedance is lower than 3.5% in this test condition. The test method used in this work can minimize measurement errors due to earth mutual impedances and ac mutual coupling. The potential difference between the grounding electrode to be measured and the potential auxiliary electrode is detected by the differential probe with the frequency bandwidth of 70 MHz. The detected potential signals are transmitted to the grounding impedance analyzer via the A/D converter. The grounding impedance and impedance phase as a function of the frequency of injected current are calculated and stored by the Labview program.

2.2 Simulation method

In order to calculate the ground current dissipation rates and grounding impedance, the counterpoise is modeled by the distributed parameter circuit model. The distributed

parameter circuit model is realized by EMTP and the results are graphically drawn by the MATLAB program. The grounding impedance and the current dissipation rate for the counterpoise are simulated in multi-layered soil structures. The soil structure layers are divided into every 10 m sections of the counterpoise and the localized soil resistivity of each sections is inversely proportional to the average soil resistivity of each 10 m section according to the current dissipation rate at the frequency of 1 kHz. Table 1 shows the localized soil resistivity and ground resistance of five 10 m sections of the counterpoise.

Table 1. Localized soil resistivity and ground resistance of each section considering the current dissipation rate at the frequency of 1 kHz.

	0-10m	10-20m	20-30m	30-40m	40-50m
Ground resistance of each section [Ω]	27.6	36.4	31.8	35.4	28.4
Localized soil resistivity [Ω · m]	175.8	231.8	202.3	225.5	180.8

Fig. 3 shows the distributed parameter circuit model of a horizontal grounding electrode for simulation by using EMTP. The current with a magnitude of 1 A is injected into one end of the equivalent circuit and the frequency of the input current varies from 100 Hz to 1 MHz. The grounding impedance and the phase difference between the current and potential waveforms are calculated. The five current probes are set at every 10 m point of the 50 m counterpoise. The counterpoise is divided into one hundred segments and each parameter is substituted in the circuit. The values of G, L, and C are calculated from Eqs. (3), (4) and (5), respectively [13-15].

$$G = \frac{\pi}{\rho} \frac{1}{\ln \frac{2l}{\sqrt{2rt}} - 1} \tag{3}$$

$$C = \frac{\varepsilon_0 \varepsilon_r \pi}{\ln \frac{2l}{\sqrt{2rt}} - 1} \tag{4}$$

$$L = \frac{\mu_0}{\pi} \left(\ln \frac{2l}{\sqrt{2rt}} - 1 \right) \tag{5}$$

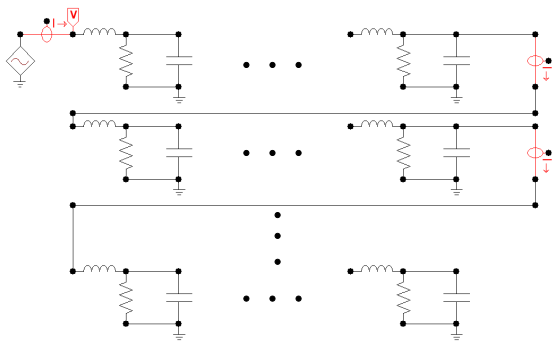

Fig. 3. Distributed parameter circuit model

When simulating the grounding impedance, it is very important to reflect the resistivity and relative permittivity of soil near the grounding electrodes. Recently, some researchers have reported the frequency-dependent soil parameters and it is important issue to simulate the grounding impedance matched with experimental results [16, 17]. In this work the frequency-dependent relative resistivity and permittivity of soil at the test site were evaluated using the soil box method presented by ASTM G57-95a [18]. The soil sample of the test site is put in the soil box and it is regard as *RC* parallel circuit.

The relative resistivity of soil is calculated as a ratio of the value measured at a given frequency to the resistivity of soil at the frequency of 100 Hz. Fig. 4 shows the frequency-dependent relative resistivity and permittivity of soil sampled at the test site. As the test frequency is increased, the relative resistivity of soil is decreased to around 60 % at the frequency of 1 MHz. The relative permittivity of soil is very high value in a low frequency and it converges to the value of some tens in the frequency of higher than 10 kHz. The simulated result of grounding impedance is rarely affected by the relative permittivity of soil in the frequency of lower than 10 kHz[17]. The measured results of the relative resistivity and permittivity

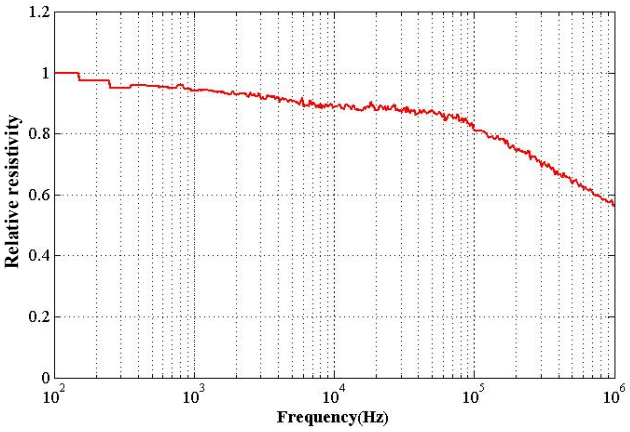

(a) Relative resistivity

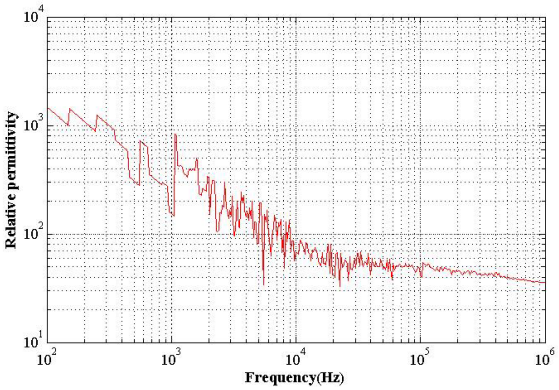

(b) Relative permittivity

Fig. 4. Measured frequency-dependent soil parameters

of soil are similar with those of other researches[16, 17, 19]. When the conductance is calculated from Eq. (2), the actual soil resistivity is yielded by multiplying the soil resitivity at 100 Hz by the relative resistivity and the measured relative permittivity of soil is used in calculation of the capacitance at a given frequency.

Distributed circuit parameters of the counterpoise are calculated by Eqs. (3), (4) and (5) using Matlab program. The EMTP(Electromagnetic Transient program) is linked with Matlab program to apply the distributed parameters automatically to the equivalent circuit model in EMTP. The distributed parameter circuit model is implemented by EMTP as shown in Fig. 3.

3. Results and Discussion

3.1 Ground current dissipation rates

The frequency-dependent ground current dissipation rates are analyzed by the measurement of the current dissipating through the grounding electrode into the earth. Fig. 5(a) shows the measured results of the ratio of the ground current dissipating into every 10 m sections of the counterpoise to the injected current as a function of the frequency of test current. The ground current of about 22 % of the injected current in the frequency of lower than 20 kHz is dispersed into the 0-10 m and 40-50 m sections of the counterpoise, respectively. On the other hand, the ground current of about 17 % is discharged at the 10-20 m and 30-40 m sections, respectively. These different current dissipation rates in the frequency of less than 20 kHz are caused by the differences of the localized soil resistivity at each sections buried in the counterpoise.

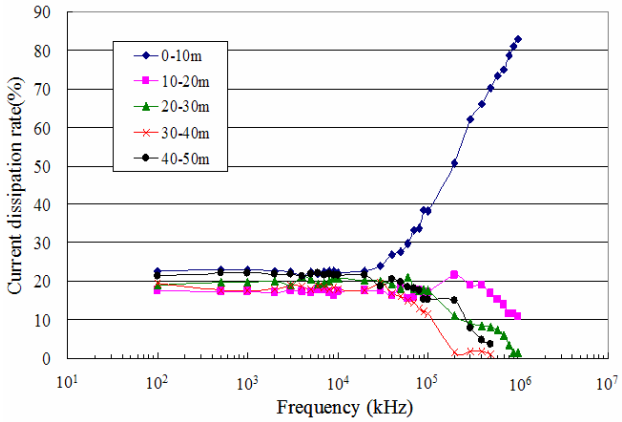

(a) Measured results

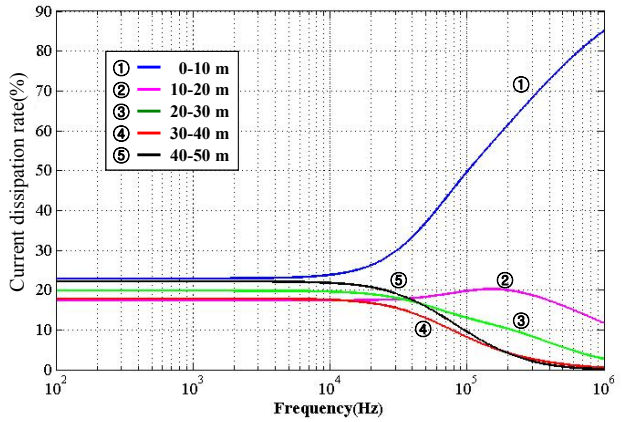

(b) Simulated results

Fig. 5. Current dissipation rates in every 10 m section of the 50 m counterpoise

As shown in Fig. 1, the soil resistivity at the sections of the 0-10 m, 20-30 m and 40-50 m of the counterpoise are relatively lower than those at the section of the 10-20 m and 30-40 m. So the low frequency ground current is easily dispersed into the soil at a place with low resistivity. The ground current dissipation rates at each sections of the counterpoise are indifferent in the frequency range of lower than 20 kHz. However, the ground current dissipation rate of the 0~10 m section begins to increase at the frequency of 30 kHz and is over 50 % at the frequency of 200 kHz and approaches about 83 % at 1 MHz. On the other hand, the dispersed current rates at about 30 kHz are beginning to decrease in the order far away the current injection point. As the frequency of injected current is increased, the dispersed current rates are decreased to the level of lower than 10 % in the order of 40-50 m, 30-40 m and 20-30 m sections. The ground current dissipation rate at the section between 10-20 m is slightly increased in the frequency of lower than 200 kHz, but it also decreases above 200 kHz. i.e., the high frequency ground currents could not flow along a long counterpoise.

The simulation of the ground current dissipation rates based on the multi-layered model reflecting the frequency-dependent soil parameters are also carried out as a function of frequency and the results are shown in Fig. 5(b). In the frequency range of lower than 10 kHz, the ground current dissipation rates at each section of the counterpoise are unchanged and are nearly same with the experimental results. As the frequency of injected current is increased over the range of some tens of kHz, the ground current dissipation rate at the 40-50 m section that gives relatively high value in the frequency of a few tens of kHz is sharply decreased. Over the frequency range of 100 kHz, the ground current dissipation rates are reduced in the order far away the current injection point. Approximate 85% of the injected current is dissipated in the 0-10 m section of the counterpoise at the frequency of 1 MHz. It was found that the ground current dissipation rates simulated by applying multi-layered soil structure are in good agreement with the experimentally-measured results.

Therefore, the low frequency ground current is largely discharged into the section of grounding electrode buried in soil with low resistivity. On the other hand, as the frequency of the injected current is increased, the ground current dissipation rates are increased near the current

injection point and are decreased at far-off place from the current injection point

3.2 Frequency-dependent grounding impedances

To investigate the characteristics of the frequency-dependent grounding impedance related to the ground current dissipation rates, the grounding impedance and phase difference between the current and potential waveforms are measured as a function of the length of counterpoise. In order to adjust the length of counterpoise, 10 m of the grounding electrode is cut from one end of the counterpoise after the grounding impedance is measured.

Table 2. Localized soil resistivity and ground resistance as a function of the length of counterpoise.

	10 m	20 m	30 m	40 m	50 m
Ground resistance [Ω]	27.60	16.70	12.34	10.01	8.55
Apparent soil resistivity [Ω · m]	175.83	186.56	192.88	199.11	205.34

The ground resistance and apparent soil resistivity calculated from Eq. (1) for five counterpoises are tabulated in Table 2. The longer the length of the counterpoise is, the lower the ground resistance is. The average apparent soil resistivity, as shown in Table 2, is increased as the length of counterpoise increases.

Fig. 6(a) shows the measured results of frequency-dependent grounding impedance as a function of the length of counterpoise. The grounding impedances measured at the frequency of 100Hz are nearly equal to the ground resistance measured by the commercial earth tester working at 128 Hz. It was known that the reactive component of the grounding impedance at 100 Hz is insignificant since the ground resistance is the real part of grounding impedance.

The greater the length of counterpoise is, the lower the grounding impedance is, when the frequency of test current is less than 20 kHz. As the frequency of injected current is increased, the grounding impedance of the counterpoise of 50 m long is greater than that of 40 m counterpoise in the frequency range from 30 kHz to 100 kHz. The grounding impedances of 40 m and 50 m counterpoise are almost same over the frequency of 100 kHz. In the same manner, the grounding impedances of the 40 m and 50 m counterpoises are greater than that of 30 m in the frequency of 40 kHz and converge to that of 30 m over the frequency of 200 kHz. As the frequency of injected current is increased, the grounding impedance of long counterpoises increases sharply and then converges to those of short counterpoises. On the other hand, the grounding impedance of the 10 m counterpoise slightly decreases in the frequency of lower than 200 kHz and gives capacitive aspect. The 10 m counterpoise appears the lowest grounding impedance over the frequency of 300 kHz

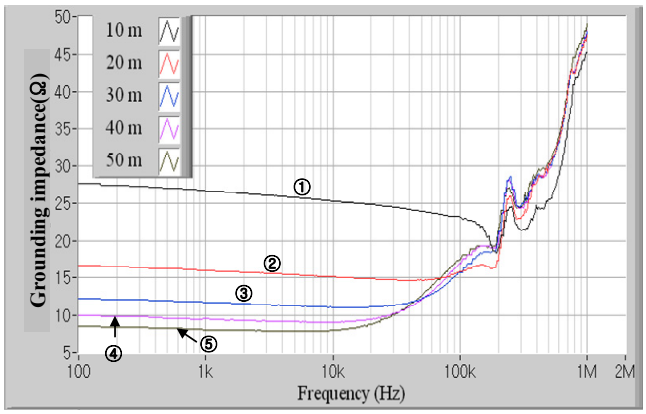

(a) Measured results

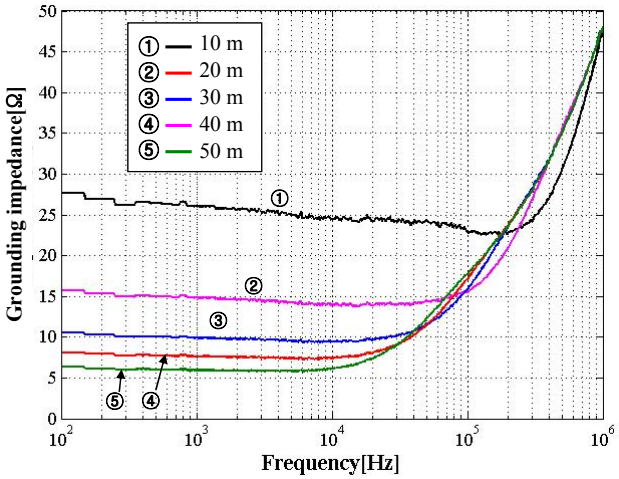

(b) Simulated results

Fig. 6. Frequency-dependent grounding impedance and impedance phase as a function of the length of counterpoise.

The distributed parameter circuit model reflecting the frequency-dependent resistivity and permittivity of soil was used in theoretical calculation of the frequency-dependent grounding impedances. The grounding impedances related to the length of counterpoise are simulated for the multi-layered soil structures and the results were shown in Fig. 6(b). As if the experimental results were shown, the longer the length of counterpoise is, the lower the grounding impedance is in the frequency range of a few tens of kHz. However, the grounding impedance of long counterpoise is increased with increasing the frequency of injected current and is greater than that of short counterpoise over the frequency of 30 kHz.

The frequency-dependent grounding impedance are affected by the ground current dissipation rates. When the current dissipation rate in the section between 40-50 m begins to decrease, the grounding impedances of 40 m and 50 m counterpoises are almost same over the frequency of

about 20 kHz. The counterpoises of longer than 30 m show same grounding impedances over the frequency of about 50 kHz when the grounding current dissipation rates in the section between 20-30 m begin to decrease. However, the grounding impedance of the 20 m counterpoise is lower than those of counterpoises of longer than 20 m at the frequency of about 100 kHz because the current dissipation rate at the section of 10-20 m is slightly increased. Owing to the decreased current dissipation rate in the 10-20 m section of the counterpoise, the grounding impedances of all counterpoises of longer than 20 m long are nearly same over the frequency of 300 kHz. Because the ground current dissipation rate into the 0-10 m section is continuously increased up to 1 MHz, the grounding impedance of the counterpoise of 10 m long gives the lowest value over the frequency of 300 kHz. i.e., in the case that the frequency of ground currents is higher than 300 kHz, the grounding system made by the grounding electrodes of less than 10 m long is much effective. Because the ground current for counterpoise of longer than 30 m did not reach to the far end of the counterpoise over the frequency of a few hundred kHz, the grounding impedance is irrespective of the length of counterpoise.

As a consequence, the grounding impedance of long counterpoises converges to that of short counterpoises when increasing the frequency of injected current since the section dispersing high frequency ground current is restricted nearby the current injection point. It is ineffective to design grounding systems with extended grounding electrodes to decrease the grounding impedance.

Fig. 7 shows the measured and simulated frequency dependent impedance phase associated with the length of counterpoise. The impedance phases increase in the order of the length of counterpoise. The measured impedance phases of the counterpoises of 20 m ~ 50 m long are almost same over the frequency of 200 kHz, and the counterpoise of 10 m long represents same grounding impedance phase with others over the frequency of 600 kHz. The positive impedance phase means an inductive characteristic and causes the increase of grounding impedance as the frequency of ground current increases. On the other hand, the negative impedance phase means capacitive characteristics and indicates the decrease of the grounding impedance with increasing the frequency of ground current. The simulated results of frequency-dependent impedance are also similar with the measured results except for the resonance oscillation occurred in the frequency range from 100 kHz to 300 kHz.

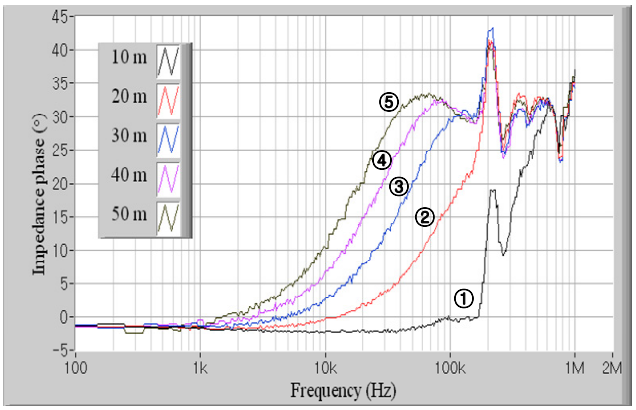

(a) Measured results

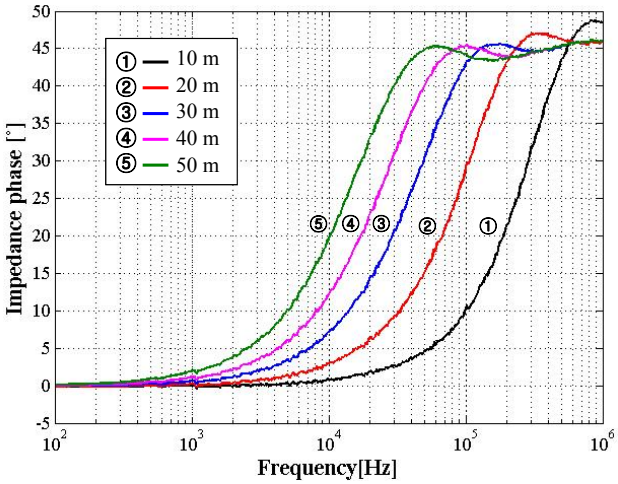

(b) Simulated results

Fig. 7. Frequency-dependent impedance phase as a function of the length of counterpoise

4. Conclusion

The frequency-dependent grounding impedances and the ground current dissipation are measured and simulated rates as a function of the length of counterpoise. The results could be summarized as follows:

The current from grounding electrode into the earth is dissipated depending on the localized soil resistivity in the frequency of a few tens of kHz. On the other hand, the ground current dissipation rates at the frequency of higher than 100 kHz are intensively converged near the current injection point. The longer the counterpoise is, the lower the grounding impedance is in the frequency of a few tens of kHz. However, the grounding impedance of long counterpoise is nearly equal to that of short counterpoise as the frequency of ground current increases. The new simulation method of the frequency-dependent grounding impedances using the distributed parameter circuit model was proposed. The results of grounding impedance and ground current dissipation rates calculated by applying the distributed parameters based on the frequency-dependent resistivity and relative permittivity of soil are good agreement with the data measured at the test site. The results obtained from this work could be used in design of high frequency grounding systems for lightning and switching surge protection.

References

[1] B. Nekhoul, P. Labie, F. X. Zgainski, G. Meunier, “Calculating the Impedance of a Grounding System”, IEEE Trans. on Magnetics. Vol.32, No.3, pp.1509-1512, 1996.

[2] Y. Liu, N. Theethayi, R. Thottappillil, “Investigating the validity of existing definitions and empirical equations of effective length/area of grounding wire/grid for transient studies”, Journal of Electrostatics, Vol. 65, pp.329-335, 2007.

[3] Korea Electric Association, “Korea Electrotechnical Regulation”, 2009.

[4] British Standards Institution, “Protection of structures against lightning”, BS 6651, 1999.

[5] M. Heimbach, L. D. Grcev, “Grounding System Analysis in Transients Programs Applying Electromagnetic Field Approach”, IEEE Trans. Power Del. Vol. 12, No. 1, pp. 186-193, 1997.

[6] A. Rousseau, P. Gruet, "Practical high frequency measurement of a lightning earthing system." Proc. 27th ICLP, pp.526-530, 2004.

[7] P. Llovera, J. A. LLiso, A. Quijano, V. Fuster, "High frequency measurements of grounding impedance on resistive soils", Proc. 28th ICLP, pp.727-729, 2006.

[8] B. R. Gupta, B. Thapar, "Impulse Impedance of Grounding Grides”, IEEE Trans. P.A.S., Vol. PAS-99, No. 6, pp. 2357-2362, 1980.

[9] S. Visacro, "A Comprehensive Approach to the Grounding Response to Lightning Currents", IEEE Trans. on P.D., Vol. 22 No. 1, pp.381-386, 2007.

[10] IEEE Std. 142, Grounding of Industrial and Commercial Power Systems”, pp.161-164, 2007

[11] H. Motoyama, “Electromagnetic Transient Response of Buried Bare Wire and Ground Grid”, IEEE Trans. Power Del. Vol. 22, No. 3, pp. 1673-1679, 2007.

[12] IEEE Std. 81.2-1991, “IEEE Guide for Measurement of Impedance and Safety Characteristics of Large, Extended or Interconnected Grounding Systems”

[13] M. E. Almeida and M.T. Correia de Barros, “Fundamental considerations on long ground electrodes design”, Proc. 13th ISH, pp.241-244, 2003.

[14] C. Mazzetti and D. Mukhedkr, “Impulse to impedance of buried ground wires”, IEEE Trans. PAS, Vol. PAS-102, No.9, pp.3148-3156, 1983.

[15] Bok-Hee Lee, Jeong-Hyeon Joe, Jong-Hyuk Choi, “Simulations of Frequency-dependent Impedance of Ground Rods Considering Multi-layered Soil Structures”, JEET, Vol.4, No.4, pp.531-537, 2009.

[16] C. M. Portela, J. B. Gertrudes, M. C. Tavares, J. Pissolato, "Earth conductivity and permittivity data measurements: Influence in transmission line transient performance", Electric Power Systems Research, Vol. 76, pp.907-915, 2006.

[17] S. Visacro, R. Alipio, M. H. M. Vale, C. Pereira, "The Response of Grounding Electrodes to Lightning Currents: The Effect of Frequency-Dependent Soil Resistivity and Permittivity", IEEE Trans. on EMC, Vol. 53, No. 2, pp.401-406, 2011.

[18] ASTM G57-95a, "Standard test method for field measurement of soil resistivity using the wenner four-electrode method".

[19] S. Visacro and C. Portela, “Soil permittivity and conductivity behavior on frequency range of transient phenomena in electric power systems”, Proc. ISH-87, Germany, Aug. 1987.

Jong-Hyuk Choi received B.S. degrees in Electronic Engineering from the Inha University, in 2006. He received M.S. and Ph.D. degrees in Electrical Engineering from the Inha University in 2008 and 2012, respectively. He is currently a researcher of Korea Electrotechnology Research Institute. His research interests include high voltage engineering and testing, grounding, electrical discharges and lightning protection.

Bok-Hee Lee received his Ph.D. degree in Electrical Engineering from Inha University in 1987. He has been with the school of Electrical Engineering at Inha University, Inchon, Korea, as an Assistant Professor since 1990, becoming a Professor in 1999. From 1988 to 1989, he was a post-doctoral research fellow at the Institute of Industrial Science, University of Tokyo. From Apr. 1999 to Feb. 2000, he was a Visiting Professor in the University of Cincinnati. His research interests are in the area of lightning, lightning protection, grounding systems, surge protection, electrical discharges, high voltage engineering and electromagnetic compatibility.

Seung-Kwon Paek received his B.S. degree in Electronics Engineering from Inha University in 1979 and his Ph. D degree in Electronics Engineering from Keio University, Japan in 1989. He has been with the Department of Electronics and Intelligent Robotics Engineering at Inje University, Kimhae, Korea as a Professor since 1991. His research interests are in the area of Plasma Measurement Image Processing, lightning Signal Image Processing.